1 Introduction

1.1 Overview of the Work

Nowadays energy markets are dominated by a substantial increase in energy demand due to the strong economic growth in the developing countries in all over the world [1]. Energy demand pattern up to the year 2050 and energy consumption pattern in India is shown in **Figure1.1** [2,3]. There are many sources of energy like traditional sources of energy, fossil fuels, nuclear sources of energy etc. Traditional energy sources have low efficiency and no longer in use. Limited fossil fuel reserves and continuous ecological degradation compelled governments and industries all around the world to look for renewable energy sources and technologies for power production [4,5]. Nuclear power is a relatively clean form of energy and may be suitable for large-scale power stations [6]. But, the major concern is its high-level radioactive waste. On the other hand, alternate energy resources are considered a long-term solution to the world's future energy demands, since they are environment-friendly and independent of our declining limited natural resources.

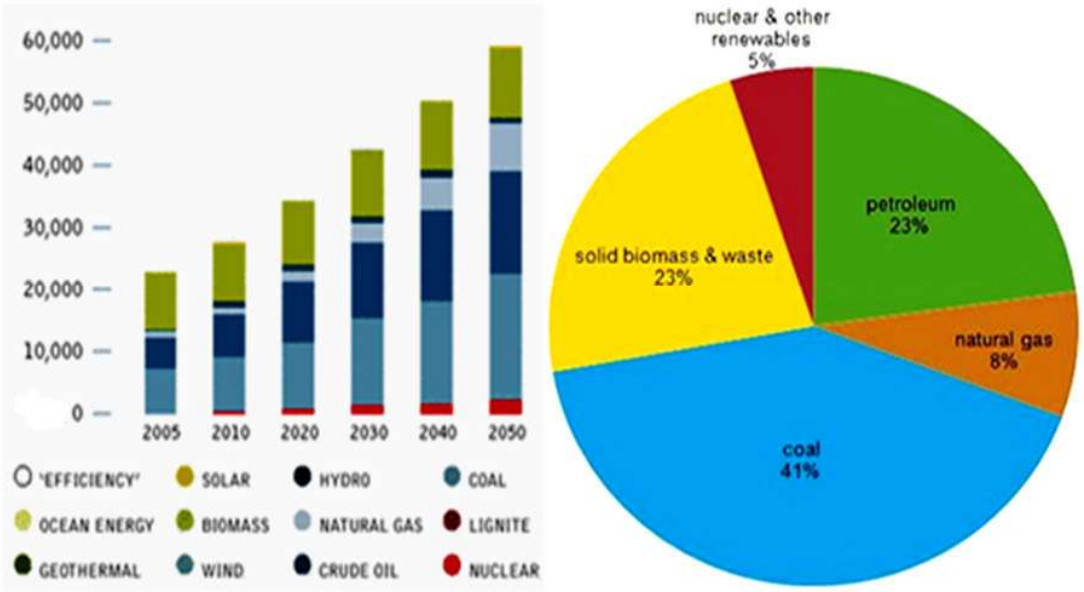

Figure 1.1 Energy demand (in Joule) and its consumption [Source: maritime executive.com]

There are several alternative and renewable energy based technologies are being developed like solar, wind, tidal, biomass, hydroelectric, ocean and geothermal technologies etc. But, these alternate energy technologies have some limitations [7] and difficulties with the stability of their energy as source, for example, on a cloudy or windless day. Their applications are somewhat limited due to lack of portability; a windmill is not much helpful to the power plant of a diesel truck, a solar panel fails to provide power at night, etc. Due to the limitations of these alternative energy sources it is better to look for sufficiently develop renewable energy resources. Among the available renewable energy sources & energy conversion devices, a fuel cell is an emerging technology for efficient and clean power generation [8]. A fuel cell is an electrochemical energy conversion device, which converts chemical energy of the fuels directly into the electricity. However, environmental issues have played a major role and emphasized one of the major strengths of the desire to use fuel cells.

1.2 Fuel Cells: an overview

A fuel cell is an electrochemical device that converts chemical energy (of fuels such as hydrogen, methane, butane or even gasoline and diesel) into electrical energy by exploiting the natural tendency of oxygen and hydrogen to react [8]. It is a simple device, containing no moving parts and only four functional components: anode, cathode, electrolyte, and interconnect. Since the energy is generated without combusting the fuel, the environmental benefits are significant.

In 1962, first time, by scientists at Westinghouse Electric Corporation (now Siemens Westinghouse), a revolution in energy research occurred due to the demonstration of the feasibility of extracting electricity from a device called a “solid electrolyte fuel cell”. Sir William Grove discovered the fuel cell principle and until the advent of space-travel was

mainly a laboratory curiosity. Fuel cells were looked upon as a safer and more reliable method to supply power than other more potentially dangerous technologies in outer space, i.e., nuclear power and the fear of environmental contamination in the event of a failed launch or re-entry. Major in-roads in the development of low cost fuel cells, escalating costs of existing power generation and fuel resources have brought fuel cell technology to the forefront, as our next technological revolution. The future international market for fuel cell systems in transportation, power generation and all other energy sectors is potentially huge [9].

1.3 Types of Fuel Cell

Fuel cells are classified on the basis of electrolyte they employed. A few of the most promising types of fuel cell and their comparison is described in Table 1.1.

Table 1.1 Comparison between different types of fuel cells.

Fuel Cell Systems	**Electrolytes**	**Operating Temperature**	**Fuel Supply**	**Application with efficiency**
Polymer Electrolyte Membrane (PEMFC)	Immobilized, acidic, polymer	RT to 200 °C	Liquid ethanol	Small Units, up to automobiles (50-55%)
Alkaline Fuel Cell (AFC)	Circulating liquid or Matrix as KOH	RT to 200 °C	Hydrogen or NH_3	Small Units and automobiles (50-55%)
Phosphoric Acid Fuel Cell (PAFC)	Concentrated acid gel	160 to 220 °C	Hydrogen or Converter	Power Plants 50 to 200 kW (40-50%)
Molten Carbonate Fuel Cell (MCFC)	Molten salt as nitrate, sulphate carbonates	600 to 620 °C	Hydrogen, CO, Natural gas, propane	Power Plants up to Mega-W (45-50%)
Solid Oxide Fuel Cell (SOFC)	Doped and Co-doped Ceria and YSZ	500 to 1000 °C	Natural gas or propane	Small to Large Power Plants (45-60%)

The above table reflects the kind of chemical reactions that take place in the cell, the kind of catalysts required, the temperature range in which the cell operates, the fuel required and other factors. These characteristics, in turn, affect the applications for which these cells are most suitable. Among the aforementioned types of fuel cells, solid oxide fuel cells have gained much attention during in last few years because use of stable solid electrolyte, robustness and high efficiency in comparison to others [8, 9].

1.4 Solid Oxide Fuel Cell (SOFC)

1.4.1 General Introduction

Fuel cells are electrochemical devices which convert directly chemical energy present in fuels into electrical energy. They are a promising alternative to traditional power generation with high efficiency and low environmental impact. Since the intermediate steps of producing heat and mechanical work typical of most conventional power generation methods are avoided, fuel cells are not limited by thermodynamic limitations of heat engines such as the Carnot efficiency. Fuel cells differ from conventional rechargeable batteries. As long as the fuel and oxidant are supplied to the electrodes, the cell will continue to produce an electric current flowing from the anode (the negative electrode) to the cathode (positive electrode), as opposed to stored chemical energy. Fuel flexibility has been demonstrated using natural gas, biogas, coal gas *etc*. Fuel cells have a potentially wide variety of applications, such as transportation, stationary power plants, micro power generation, *etc*. Transportation markets worldwide have exhibited remarkable interest in fuel cells. Nearly all major vehicle manufacturers and energy providers are supporting their development [10].

Among the various kind of fuel cells, Solid Oxide Fuel Cells (SOFCs) are promising and potential breakthrough tool for the low cost production of electricity in comparison with

currently available fossil fuels because of increased demand for high quality and reliable energy with increasing expectations for environmental sensitivity [8]. In SOFCs, it is possible to achieve an electrochemical reaction at the electrodes simply by supplying fuel and air without using expensive noble metal catalysts. Solid oxide fuel cells (SOFCs) are comprised of a layered structure of a dense electrolyte sandwiched between porous and permeable electrodes (anode and cathode) [8]. In addition to that, such fuel cells provide the highest energy conversion efficiency and excellent fuel flexibility. However, several of the challenges hinder SOFC technology which are a consequence of the high temperature (900-1000°C) required for their operation. This high temperature is used to overcome limitations of ionic conductivity in available solid electrolytes and of kinetics in available electrode materials [11]. The high operating temperature places severe constraints on materials selection, implies difficult fabrication processes, induces materials over cost and reduces thermal cycling and fuel cell life.

In recognition of these challenges, there are presently major research efforts ongoing to decrease the operating temperature of SOFC to moderate temperatures, *i.e.* from 500 to 800°C. Therefore, research has been focused on improving electrolyte material conductivity because a major part of fuel cell resistance is derived from the electrolyte resistance. Many families of oxygen conducting compounds have been thus explored but very few present at the same time good mechanical properties, chemical stability in both oxidative and reducing atmospheres, good ion conduction and poor electronic conduction. Another strategy consists in exploring proton conducting materials since the transport of protons is generally a low-activation energy process. This implies that the conductivities of compounds based upon proton conduction might be higher than that of compounds based upon oxygen ion conduction at low temperature. **Figure 1.2** illustrates this point showing the comparison of the conductivities of well-known proton and oxide ion conducting oxides at different temperatures [12].

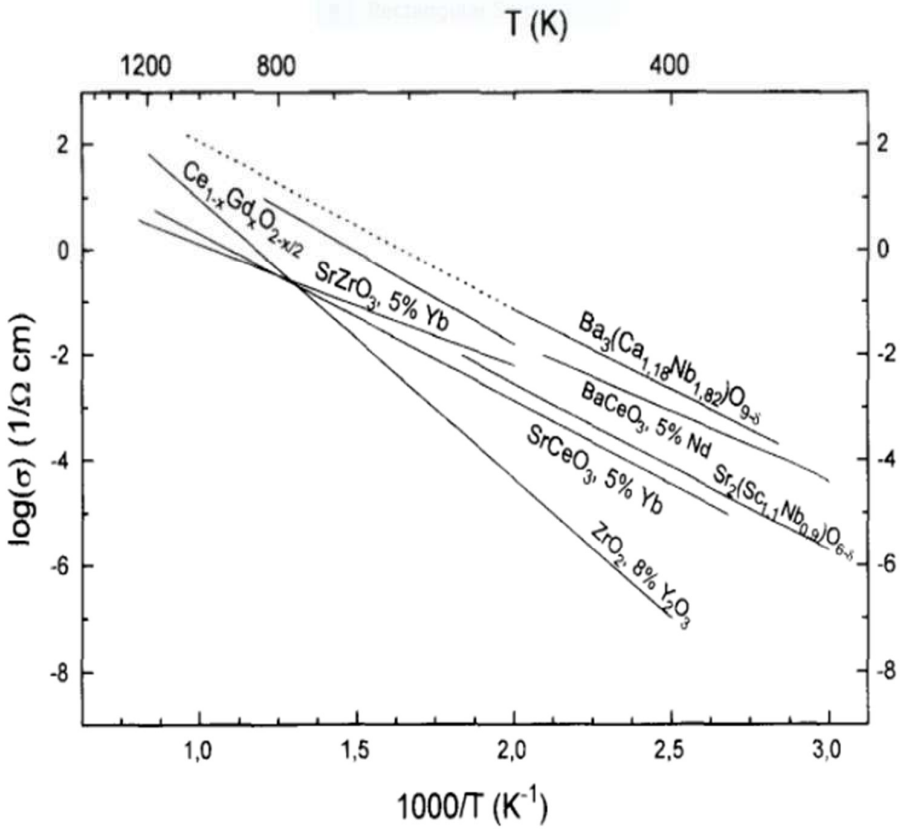

Figure 1.2 Conductivity of some solid electrolyte oxides for SOFCs [12]

Iwahara *et al.*[13, 14.] first explained the existence of proton conduction in ABO_3 perovskite compounds at elevated temperature and then many families of compounds have been explored such as acceptor-doped perovskites oxides, binary rare earth oxides with fluorite-related structures or ternary oxides with pyrochlore structure. The experiments demonstrate that the highest proton conductivities are observed for perovskites oxides [15]. Electrical power generation systems based on SOFC have the following advantages:

- High power generation efficiency
- High thermal efficiency
- Long term performance and stability
- Combined heat and electricity generation for industrial and domestic applications.

- Capable of operating on a wide variety of hydrocarbon fuels
- SOFC has a solid electrolyte, which eliminates the corrosion and liquid management problems of the PAFC and MCFC

Furthermore, SOFC system efficiencies can be improved by the internal reforming of natural gas within the fuel cell stack [16]. With modular construction, it is possible to adapt SOFC systems to suit the load required and as long as fuel is present, the SOFC is able to continually operate in almost any environment.

1.4.2 Operation of Solid Oxide Fuel Cells

Figure 1.3 shows schematically how a solid oxide fuel cell and proton conducting fuel cell work. The cell is assembled with an electrolyte sandwiched between two porous electrodes. Air flows along the cathode (which is therefore also called the "air electrode").

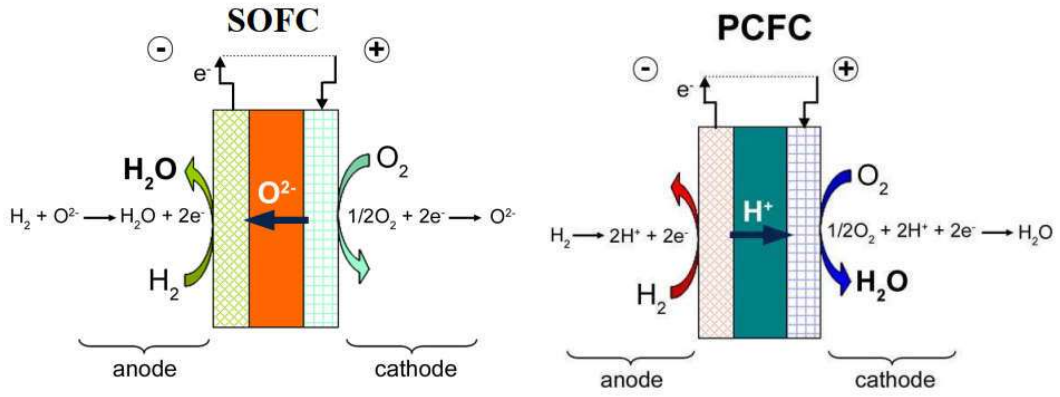

Figure 1.3 Working principle of unit cell of solid oxide fuel cell (SOFC) and proton conducting fuel cell (PCFC) [Ref: researchgate.net]

In a classical SOFC based on anion-conducting electrolyte, the reduction of oxygen occurs at the cathode and the resulting O_{2-} anion is then transported across the electrolyte till the anode side where it will combine with H_2 gas to form gaseous water. The two half reactions of

oxidation/reduction involve exchanges of electrons that circulate in the external circuit. In Proton Conducting Fuel Cells (which is actually a kind of SOFC), hydrogen is oxidized into H^+ and this H^+ is carried out till the cathode through the proton conducting electrolyte. H^+ ions thereafter react with O_2 gas to form gaseous water. Intrinsically, the oxide ion-conducting fuel cell generates then water vapour on the anode side which lowers the cell voltage and reduces fuel utilization which requires considerable fuel circulation [11]. On the other hand, a proton conducting fuel cell produces water at the cathode. The high air flow usually used takes care of this while the anode fuel gas remains undiluted by water vapor, keeping the Nernst voltage high [17].

The major problem of ceramic proton conductors is their rather basic nature because Sr and Ba are often some of their components [17]. Thus, they are vulnerable to destructive reaction with acidic gases such as CO_2 or SO_2/SO_3, especially at moderate temperature and may also react with water at moderate and low temperatures to form hydroxides. All in all, proton conducting oxides are advantageous in intermediate or low temperature and can be candidates for electrolyte materials for reducing the operation temperature of SOFCs

1.5 Materials Selection for the Component of SOFC

The material selection requirements for SOFC are quite challenging, stubborn and well established. On the basis of the characteristics of cell as oxygen-ion conductor, electronic conductivity, stability in both oxidizing and reducing conditions, density and fuel flexibility there are following essential components:

1.5.1 Electrodes (Cathode and Anode)

The main two electrodes are anode and cathode by which electrolyte was sandwiched in the cells. Cathode acts in oxygen atmosphere where oxygen molecules dissociated into

oxygen ions to reach the electrode/electrolyte interface. In some designs (e.g. tubular) the cathode contributes over 90% of the cell's weight and therefore provides structural support for the cell [18]. Due to the strong oxidizing atmosphere at high temperature, it's not easy to choose lower cost metals. Any reduction in operating temperature lowers the operating costs and expands the materials selection, creating an opportunity for additional cost savings. The challenge is to sinter the cathode adequately, often by co-sintering with the other components while maintaining sufficient interconnected porosity.

The anode must meet most of the same requirements of the cathode for electrical conductivity, thermal expansion compatibility, porosity and has to function in a reducing atmosphere. The reducing atmosphere combined with electrical conductivity requirements makes the system as attractive candidate materials. In order to maintain porosity, pore formers such as starch, carbon, or thermosetting resins are added. These burn out during firing and leave pores behind. Mostly development has been focused on nickel due to its abundance and affordability. The main requirements of the SOFCs electrodes are [8, 19, 20] High electronic and less ionic conductivity

- Porous structure optimized for the mass transport of the gas species
- Thermal expansion compatible with those of the other cell components
- Chemically inert
- Resistance to thermal cycling
- High catalytic activity and good mechanical strength
- Good adherence to the other cell components and porosity
- Minimum inter-diffusion and Low volatility
- A superficial resistivity (≤ 0.2 ohm/cm^2)
- Moderate materials and fabrication cost

The polarization loss occurs at electrodes due to voltage drop as low operating temperature.

Major cathode materials: Doped lanthanum cobaltite & manganite (LSC & LSM), (LSM-YSZ) composite, Lanthanum-Barium cobaltite (LBC), $Pr_{0.6}Sr_{0.4}MnO_{3\pm\delta}$ (PSM) etc.

Major anode materials: Porous Ni, NiO/YSZ, NiO/SDC, La doped Strontium titanate (LST), Ni-Cu-YSZ, $Ba_{0.5}La_{0.5}Ti_{0.3}Mn_{0.7}O_3$, etc.

1.5.2 Interconnect

Just as an internal combustion engine depends on several cylinders to provide enough power to be used alike fuel cells in combination in order to generate enough voltage and current. This means that the cells need to connect together and a mechanism for collection of electrical current needs to be provided, hence the need for interconnects. The interconnect functions as the electrical contact to the cathode while protecting it from the reducing atmosphere of the anode. The high operating temperature of the cells combined with the severe environments means that interconnects must meet the most stringent requirements of all the cell components [20]:

- ✓ 100% electronic conductivity, no porosity (to avoid mixing of fuel and oxygen).
- ✓ Thermal expansion compatibility and inert with respect to the other fuel cell components.
- ✓ It will be exposed simultaneously to the reducing environment of the anode and the oxidizing atmosphere of the cathode.
- ✓ Absence of mass transport effects in the presence of chemical gradients that may lead to the formation of voids or high contact resistances
- ✓ No time dependent phase change
- ✓ Low material and fabrication cost

For YSZ based SOFC operating at about 1000 °C, $LaCrO_3$ doped with an alkaline earth element (Ca, Mg, Sr, etc.) is used as interconnect to improve its conductivity. Ca-doped yttrium chromite has considered also because it has better thermal expansion compatibility, especially in reducing atmospheres. Recently, Ferritic stainless steel (FSS) with minor additions of Nb and Ti elements has been carried out at 800 ºC in an air for 70 cycles.

1.5.3 Electrolyte

The main component in the SOFC is the solid electrolyte. The function of the electrolyte is to transport the oxygen ion without significant losses from the cathode to the anode. The transport of oxygen ions in the electrolyte occurs through the oxygen vacancies in the oxygen sub-lattice. The concentration of vacancies and their mobility determines the electrolyte conductivity. Among the number of suitable oxide ion conductors, high oxygen diffusivity has been observed in oxides which exhibit large tolerance for atomic disorder.

In the cell, oxygen molecule has been converted into oxygen ions that must migrate through the electrolyte to the fuel side. For the migration of oxygen ions, electrolyte must satisfy the following criteria [8, 19, 20]:

- The electrolyte must possess a high ionic conductivity and no electrical conductivity.
- It must be fully dense to prevent short-circuiting of reacting gases throughout it.
- It should be thin also to minimize resistive losses in the cell.
- As with the other materials, it must be chemically, thermally and structurally stable over a wide range of temperature.

***Major electrolyte materials*:** Yttria stabilized Zirconia (YSZ), Sm/Gd doped ceria (SDC/GDC), Sr & Mg doped Lanthanum gallate (LSGM), Li doped CGO (Li-CGO), tri-doped ceria $Ce_{1-x}(Pr_{1/3}Sm_{1/3}Gd_{1/3})_xO_{2-\delta}$ etc.

The main difficulty which limits the operation of these components is their high operating temperature range from 800 °C to 1000 °C [21]. This high temperature decreases the cell life time and increases the cost of materials. It is also necessary to identify new electrode-electrolyte materials in order to be able to decrease the operating temperature of the SOFC so that inexpensive manifolding materials can be used and the cost of the initial thermal energy required to heat the cells can be lowered. Lowering the temperature can significantly improve the thermal expansion incompatibilities. However, by lowering the operating temperature of the fuel cell, the ionic conductivity of the electrolyte is significantly decreased. Therefore, for the fuel cell output at intermediate-temperatures are favourable than the output observed at higher temperature.

1.6 High and Intermediate Temperature Solid Oxide Fuel Cell

1.6.1 High Temperature Solid Oxide Fuel Cells (HT-SOFC)

The enhanced efficiency of SOFC in comparison with other energy conversion systems is borne out by its high operating temperature exceeds 800 °C. The components for HT-SOFCs are the following:

- ✓ Electrolyte: 8-mol % yttria stabilized zirconia (YSZ)
- ✓ Anode: Ni-YSZ cermet
- ✓ Cathode: Sr doped lanthanum manganite (LSM)
- ✓ Interconnect: Doped lanthanum chromate (LCR)

1.6.2 Demerits of High Temperature Solid Oxide Fuel Cells

Although the power output is high, HT-SOFC suffers with some serious demerits. Material costs are high, particularly for interconnect and construction materials. For high temperature SOFC, a ceramic such as lanthanum chromite is used as interconnect, or, if the temperature is limited to <1000 °C, a sophisticated refractory alloys e.g. based on mechanically

alloyed Y/Cr can also be utilized for interconnect. In either case interconnect represents a major proportion of the cost of the stack. A potential drawback to the use of chromium containing ceramics and alloys is the volatility of the material which can result in contamination of the stack components. This has an increased significance for future reclamation of materials and components from using stacks where the presence of a toxic material such as Cr^{6+} would require special disposal procedures.

1.6.3 Intermediate Temperature Solid Oxide Fuel Cells (IT-SOFC)

Operation of the SOFC between the temperatures range 500-600 °C, termed as Intermediate Temperature Solid Oxide Fuel Cell (IT-SOFC) and can overcome some of the problems of High Temperature Solid Oxide Fuel Cell. The new generation of electrolytes such as Gd-doped ceria (CGO), Sr and Mg doped lanthanum gallate (LSGM) which possess much higher oxide ions conductivity at temperature below 600 °C with respect to YSZ electrolyte is considered as promising electrolytes.

1.6.4 Merits of Intermediate Temperature Solid Oxide Fuel Cells

Due to low Operating temperature below 600 °C, IT-SOFC offers several benefits. Some of the salient features are pointed below:

- Operation at less than 600 °C means that low cost metallic materials, e.g. ferritic stainless steels or even metal-alloys can be used as interconnect and construction materials. This makes both the stack and balance of plant cheaper and more robust.
- Lower temperature operation offers the potential for more rapid start up and shut down procedures.
- Reducing the operating temperature simplifies the design and materials requirements of the balance of plant.
- Low operating temperature significantly reduces corrosion rates.

In order to operate at reduced temperatures, several changes need to be made to cell and stack design, cell materials, reformer design & operation and operating conditions.

The present work has been focused on electrolyte material of SOFC at intermediate temperature range. Since electrolyte must possess a high ionic conductivity, discussed earlier, therefore it is necessary to discuss the factors that affect the ionic conduction through the material.

1.7 Factors Influencing Ionic Conduction of the Electrolyte

In the electrolyte materials, optimizing the ionic conductivity is of more importance. The ionic conductivity of electrolytes can be influenced by many parameters. There has been made an enormous effort for the improvement of ionic conductivity of the electrolyte. Composition, microstructure and processing are fully related to each other in the electrical properties [22, 23]. A relation between these factors and ionic conductivity of the oxide electrolyte is shown below in **Figure 1.4**.

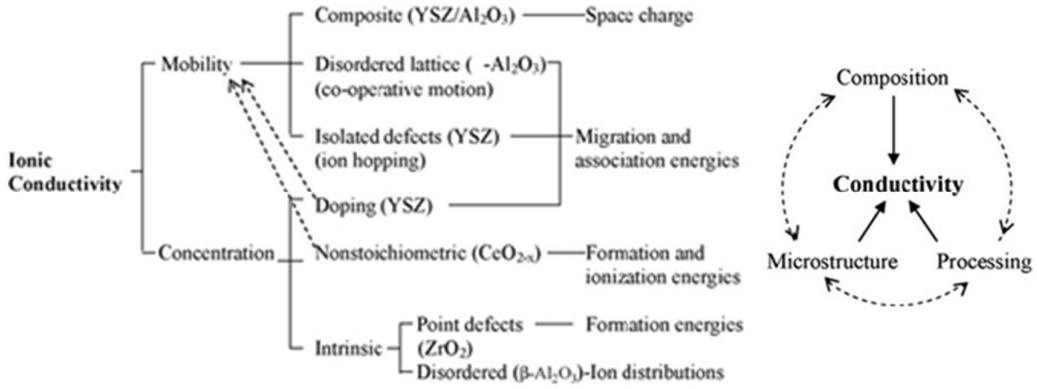

Figure 1.4 (a) The major sources of ionic carriers in oxides and their respective mobilities compiled from literatures **(b)** The correlation of composition, microstructure, processing and electrical conductivity in polycrystalline materials under given temperature and surrounding atmosphere [24].

Hence, the following factors can enhance the conductivity of electrolyte

- Doping and multiple doping can improve the ionic conductivity. The ionic conductivity of electrolytes can be maximized through composition modification by selecting an alio-valant and iso-valent dopant with suitable ionic radii and its concentration [25].
- Introducing a second phase to form a composite electrolyte may change grain boundary and therefore vary the electrical conductivity of the electrolytes [26].
- Properties of grain boundaries such as impurity segregation and space charge play an important role in the ionic conductivity [27].
- Processing conditions also influence the final ionic conductivity depending on density, the level of impurities, thermal history and formation of micro domain [28].

Out of these factors, there are some other parameters which directly or indirectly affect the ionic conductivity.

Since, ionic motion is the action of ions hopping under the influence of an electric field through the lattice via defects. The rate of ion conduction is described by very common **Eq. (1.1)** [29, 30].

$$\boldsymbol{\sigma = nq\mu} \tag{1.1}$$

σ is the ionic conductivity ($S.cm^{-1}$), n is the number of mobile ions in a given volume of lattice (cm^{-3}), q is the magnitude of the charge for the oxygen ion (coulombs) and μ is the mobility of the ions ($cm^2\ sec^{-1}\ V^{-1}$). In the case of oxygen-ion conductors, conduction occurs via anion vacancies so that

$$\boldsymbol{\sigma_v = C_v q_v \mu_v} \tag{1.2}$$

where the subscript v means vacancy and C is the number of anion vacancies per unit volume (cm^3) According to the Nernst-Einstein relation, the mobility is related to diffusion constant [27], D by the equation:

$$\mu = \boldsymbol{qB = qD/kT} \tag{1.3}$$

Where B is the absolute mobility. D is given by

$$\boldsymbol{D = a^2 v_o \exp(\Delta S_m/k)\exp(-\Delta H_m/kT)} \quad (1.4)$$

Where, 'a' is the jump distance of vacancy (cm), ν_0 is an appropriate lattice vibration frequency (sec^{-1}) and ΔS_m and ΔH_m are the activation entropy (eV K^{-1}) and activation enthalpy (eV) of diffusion respectively. Since C_v is represented as:

$$\boldsymbol{C_v = [V_{\ddot{O}}]\{1 - [V_{\ddot{O}}]\}N_o} \quad (1.5)$$

Where N_o is the number of oxygen sites per unit volume, the following equations can be obtained using (1.1), (1.3), (1.4) and (1.5).

$$\boldsymbol{\sigma T = A'[V_{\ddot{O}}]\{1 - [V_{\ddot{O}}]\}\exp(-\Delta H_m/kT)} \quad (1.6)$$

$$\boldsymbol{A' = (4e^2/k)a^2 v_o N_o \exp(\Delta S_m/k)} \quad (1.7)$$

For small values of $[V_{\ddot{O}}]$ **Eq. (1.6)** can be approximated as:

$$\boldsymbol{\sigma T = A'[V_{\ddot{O}}]\exp(-\Delta H_m/kT)} \quad (1.8)$$

The enthalpy term can be replaced by a general activation energy term, $E_a$as

$$\boldsymbol{\sigma T = \sigma_o \exp(-E_a/kT)} \quad (1.9)$$

Where σ_o is a pre-exponential constant, T (K) is the absolute temperature and E_a (Scm^{-1} K) is the activation energy for oxygen diffusion. In this way temperature directly affects the ionic conductivity (σ)**.**

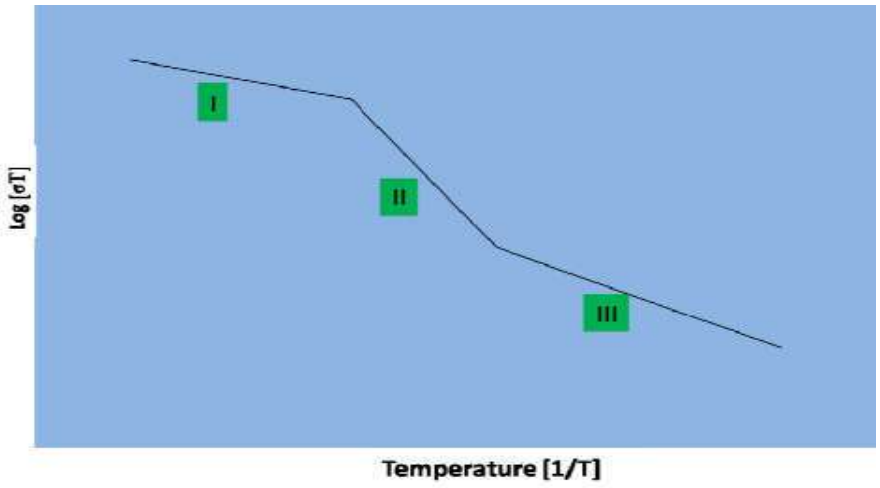

Figure 1.5 A schematic representation of the conductivity behavior of oxide ion conductor.

Arrhenius relation (temperature dependence) of the electrical conductivity of doped perovskite oxide cannot be expressed by single exponential function shown in **Eqs (1.6), (1.8)** or **(1.9)**. Generally, the usual temperature dependence electrical conductivity can be shown (see **Figure 1.5**) in the three regionable section according to kilner et al. [1982]. In first (I) region which appear at high temperature, the electrical conduction is verified by intrinsic defects (Schottky or Frenkel defect) in the crystal lattice. In second (II) region, electrical conduction is directly controlled by the majority of charge carrying defects occurred by an aliovalent dopant ions or impurity. In third (III) region, as a guideline at low temperatures, the charge carrier's majority carrying defect is determined by the thermodynamic equilibrium between the free defects and associated pairs. In the view of these fact that doped perovskite oxides have a large number of vacancies, they just have the regions II and III respectively.

1.8 Perovskite's Oxide System

The perovskite oxides e.g. $SrCeO_3$, $LaAlO_3$, $LaGaO_3$, $CaTiO_3$ etc. are very important material for SOFC, as it has generally stable crystal structure, large free lattice volume and substitution liberty [31]. The first natural perovskite calcite ($CaTiO_3$) was discovered by German chemist and mineralogist Gaustav Rose in 1839; which is known as perovskite on the name of Lev Alexeievitch Perovsky [32]. The general chemical formula belongs to this family is termed as ABX_3; where A and B are cations and X is the anion either oxygen or halide group elements. The valence of A and B is taken to be in such a way that it could be compensated by the charge of anions. Majority of elements combined in the form of (A^{3+} - B^{3+}), (A^{2+}, B^{4+}), (A^{+}, B^{5+}) from periodic table is found to be exhibit perovskite structures, e.g. $LaAlO_3$, $BaSnO_3$, $KNbO_3$ etc. The perovskite structure can be described in the framework of BO_6 octahedral which is formed by the sharing of oxygen present at the corner. In this structure the A atom is

situated at the corner position of the cube and shared by eight octahedral while B is situated at the body centred position of the cube and oxygen is present at the face of each cubic face and forms an octahedral by B-cation, as seen from **Figure 1.6**. The perovskite structure can also be understood in terms of AO rock salt layer interconnecting by two layers of BO_2 from above and below in order to describe the layer structure. The perovskite structure is one of the highest multifunctional structures in which an incredibly wide range of phases can be produced with completely different functions through structural manipulation [33].

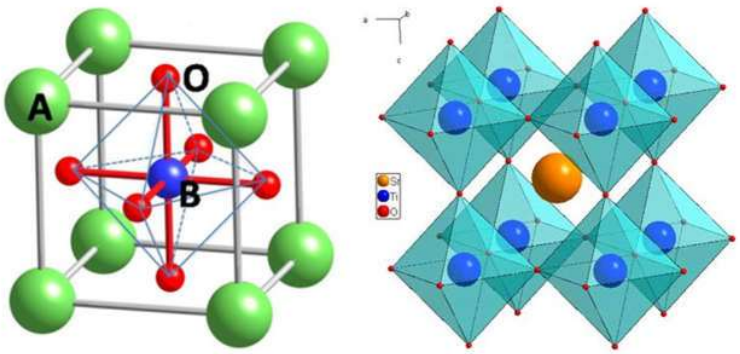

Figure 1.6 Perovskite structure ABO_3 and octahedron BO_6.

Due to the extreme flexibility of structures by replacing cation, one dimension of the compositional and structural diversity in perovskite can be sustained by the distortion created by the cation. The degree of mismatch between the layer of AO and BO_2 (determined by mismatch in ionic radii) determines the tolerance of perovskite structure [34]. The perfect geometrical match between AO and BO_2 layers give an ideal perovskite structure. Geometrically consistency is determined by the equation given as follows:

$$r\,(A-O) = \sqrt{2}\,r\,(B-O) \tag{1.10}$$

Where, $r\ (A-O)$ and $r\ (B-O)$ are the distances obtained from ionic radii of the respective atom. The persistence of structure is usually expressed in terms of the "Tolerance Factor (t)". It was first introduced by Goldschmidt which can be expressed mathematically as follow [34];

$$t = \frac{r_A + r_O}{\sqrt{2}\,(r_B + r_O)} \tag{1.11}$$

Where, r_A, r_B and r_O are the ionic radii of cation A, B and anion O respectively. Depending on the tolerance factor various crystal structures are possible, for example t=1 gives an ideal cubic structure. The other crystal structures and their tolerance factor are given in Table 1.2.

Table 1.2 Tolerance factor of different crystal structure.

Goldschmidt tolerance factor (t)	**Structure**	**Explanation**	**Example**
>1.0	Hexagonal or Tetragonal	A ion too big or B ion too small.	$BaTiO_3$[35]
0.90-1.00	Cubic	A and B ions have ideal size.	$BaSnO_3$[35] $BaTiO_3$ [36]
0.71 - 0.90	Orthorhombic/Rhombohedral	A ions too small to fit into B ion interstices.	$GdFeO_3$ [35] $CaTiO_3$ [35,37]
<0.71	Triclinic/Monoclinic	A ions and B have similar ionic radii.	Ilmenite, $FeTiO_3$ [38]

Consider an example $t = 1.002$ approaches ideal cubic structure of $BaSnO_3$ with space group $Pm\bar{3}m$. However, the variety in the perovskite structure exhibited for lower symmetry which leads for lower t as 0.8. The perovskite have $A-O$ bond under tension and $B-O$ bond under compression for $t < 1$. In order to reduce this effect, the oxygen shared corner BO_6 octahedral consistently tilt or rotate about pseudo cubic axis which accommodate smaller size of cations A in the interstices space between them [34]. Tilting in the octahedral reduces the $Pm\bar{3}m$ symmetry to lower symmetry subgroups. Using crystallographic principle, this

particular tilt in octahedral is associated with specific subgroup or class of symmetry [38]. In addition, the rotation of octahedral or distortion it leads to a change in the bond length of $B-O$ due to John-Teller distortion. The John-teller distortion has active because the cation B is belongs to the Transition metal such as Mn^{3+}, Fe^{4+}, Ni^{3+}, Cu^{2+} etc. In transition metal, each element have unpaired electron in their d shell [39, 40]. If t > 1, the A cations are too large to fit within the polyhedral framework of the BO_6 at the 12 fold site and the hexagonal polytype structure can be formed. Of particular interest related with stability of the cubic phase in $BaTiO_3$ with tolerance factor $t \approx 1.04$. Such a high tolerance factor induced a cooperative ferroelectric displacement of Ti^{4+} cations [41]. Due to presence of lone pair electrons in cations which have ns^2 core electron induced special structural effects resulted ferroelectricity. Due to steriochemical lone pair effect of Pb ions on the oxygen framework of $PbTiO_3$, it results a strong displacement of Pb^{2+} and Ti^{4+} ions from their polyhedral centres [42]. Another variant of structural diversity in stoichiometric perovskites is provided by cation ordering on either A or B - sites.

1.9 Types of Perovskite Oxides

On the basis of cation valencies (A^{m+} and B^{n+}), perovskite oxides can be divided into five categories. The basic criteria of classification of is that sum of the valencies of cations (A+B) must be equal to anions (oxygen) valencies to maintain the electro neutrality. The three categories are briefly described one by one below:

1.9.1 $A^{1+}B^{5+}O_3$ Type Structure

In this category, A-site is occupied by monovalent cation and B-site by a pentavalent cation. For example, $LiNbO_3$, $NaNbO_3$, $KTaO_3$, $KNbO_3$ and $AgNbO_3$ etc. Generally, they have ferroelectric and antifero-electric materials. $KTaO_3$ and $KNbO_3$ are used in acousto-optic and electro-optic devices while rest are used in electro-optic devices, microwave surface acoustic devices and holographic memory.

1.9.2 $A^{2+}B^{4+}O_3$ Type Structure

In this type of perovskite oxides, A-site of is occupied by divalent cations and B-site is occupied by tetravalent cations. In electro-ceramics, a number of perovskite oxides are studied by the general formula $A^{2+}B^{4+}O_3$ where A cations are alkaline earth metal (A= Sr, Ba, Co, and Pb etc.) and B cations transition elements (B=Ce, Ti, Sn, Zr, Hf, Mo, Th etc.). Some important examples of $A^{2+}B^{4+}O_3$ series are $SrCeO_3$, $CaTiO_3$, $BaTiO_3$ and $PbTiO_3$ are used as proton conductor, piezoelectric and ferroelectric materials. They are utilized as a piezoelectric transducer, phonograph pickups, air transducers, instrument transducers and ultrasonic devices.

1.9.3 $A^{3+}B^{3+}O_3$ Type Structure

In such type of perovskite oxides both A and B cation sites are occupied by trivalent cations. Where A^{3+} cation is rare earth metal ions while B^{3+} cation is a transition metal ions, respectively. Some of the well-known examples of A^{3+} $B^{3+}O_3$ type structure are $BiMnO_3$, $LnCoO_3$, $LaNiO_3$, $GdCoO_3$, $LaCoO_3$, $LaFeO_3$, $LaMnO_3$, $LaFeO_3$ and $LaCrO_3$ etc. . This type of perovskite materials is extensively studied due to their fascinating structural, electrical and magnetic properties. These are more preferred potential candidates for the cathode and interconnect in a solid oxide fuel cell.

1.10 Properties of Perovskite

It is useful to study various properties like electrical properties, magnetic properties and optical properties based on the variety of structure present in the perovskites. These properties could be improved either by substitution of dopant or by changing the processing parameters like time temperature etc. The properties of perovskites can be modified by compositional modification also; in case of compositional modification there are three types of substitution [43]. These types of substitution are discussed below;

I. **Isovalent Substitution:** In this substitution, the substituent ion has the same valency as host ion. This type of substitution may be done at either A-site, B-site or both site of

ABO_3. Therefore, no excess charge is generated by this substitution and the material becomes overall neutral. For example Ba^{2+} at Sr^{2+} site in $SrSnO_3$, Ti^{4+} at Sn^{4+} site in $SrSnO_3$ and so on.

II. Hetrovalent Substitution: In this case, the valency of the substituent ion is different from host ion. This type of substitution can also be done either at A-site, B-site or both sites. There are two types of substitutions in this category;

a) Acceptor type substitution: In this category, the substituent ion has lower valency than host ion, leading creation of excess hole or charged vacancy in the unit cell. For example, Eu^{3+} at Ce-site of $SrCeO_3$ where the following charge compensation mechanism takes place.

$$Eu_2O_3 \xrightarrow{SrCeO_3} 2Eu_{Ce}{}' + Sr_{Sr}^{x} + 3{O_0}^{x} \quad (1.12)$$

$2Eu_{Ce}{}'$ = The excess charge on a lattice is compensated by either creation of a hole or oxygen vacancies, $2Eu_{Ce}{}' = [2h\cdot] = [V_{\ddot{O}}]$

b) Donor type substitution: In this class of substitution, the substituent ion has higher valency than host ion which leads the creation of excess charge in the unit cell. For example, La^{3+}, Nd^{3+} at the Sr-site of $SrCeO_3$, the charge compensation mechanism takes place as follows:

$$La_2O_3 \xrightarrow{SrCeO_3} 2La_{Sr}{}^{\cdot} + Ce_{Ce}^{x} + 3{O_0}^{x} \quad (1.13)$$

Where, $2La_{Sr}{}^{\cdot}$ = is the excess charge on the lattice which has been compensated by either creation of electron or cationic vacancies, $[2La_{Sr}{}^{\cdot}] = [2e'] = [V_{Sr}'']$

III. Valence compensated substitution: Simultaneous substitution of a combination of hetrovalent ions at A and B sites in ABO_3, results in excess of charge carrier in the unit

cell. The resultant charges carrier in the unit cell is compensated by internal charge compensation mechanisms.

Based on the above compositional modification and charge compensation processes the properties of perovskite oxides have been modified and discussed as below;

1.10.1 Electrical properties

Generally, the synthesis of the ceramic oxides (ABO_3) has been carried out at high temperature, i.e., $\leq 1400^oC$ and at this much high temperature the loss of oxygen takes place from the lattice site which makes the site positively charged. This positively charged site maintained the charge neutrality by reduction of cation B or creation of electron which makes ABO_3 as oxygen deficient phase [43]. The presence of oxygen vacancy manipulates the oxidation state of transition metal or post transition metals. The manipulation of valance states of transition metal improved the electronic as well as ionic conductivity depending on the types of substitution [44, 45]. Most of the perovskites served as a good oxygen ion conductor and applicable in various electrochemical devices such as solid oxide fuel cells (SOFCs) [46, 45]. Rare earth (RE) based aluminates ($LnAlO_3$) doped with acceptor attracted the most significant interest since 1970 [47, 48], due to their low cost, bearable thermal expansion coefficient and higher stability with respect to volatilation compared to doped $CeO_{2-\delta}$ and $LaGaO_{3-\delta}$ [49, 50]. The maximum oxygen ion conductivity and minimum vacancy enthalpy association is improved by incorporating Sr^{2+} at the Ln site and Mg at Al site of $LnAlO_3$ site which was approximately 0.7 Scm^{-1} [51].

Piezoelectric effect is the second interesting properties in which the electric charge is created by applying pressure. It also exhibited an excellent electromechanical properties near to the morphotrophic phase boundary (MPB) compositions [52, 53]. The $PbZrTiO_3$ (PZT) is the most common piezoelectric ceramic materials which were used from last decades [52]. Ultimately, replacing of Pb-based materials is required due to environmental and toxicity issues related

with lead. Therefore, extensive studies have been reported on the lead free materials including perovskites such as $(Na_{0.5}Bi_{0.5})TiO_3$ (NBT) and $(K_{0.5}Na_{0.5})NbO_3$ (KNN) and their solid solutions [53, 54, 55.]. KNN has the piezoelectric coefficient (d_{33}) of the order of ≈ 100 pC/N [53]. With the addition of different perovskites such as $LiTaO_3$, $LiNbO_3$, $LiSbO_3$ and $SrTiO_3$ in KNN based materials; it was showing soft piezoelectric behaviour which is analogous to donor doped PZT materials. Using conventional solid state reaction for the synthesis of KNN modified materials achieved nearly full densification [53, 56, 57].

In Multilayer ceramics capacitors, Barium Titanates ($BaTiO_3$) perovskite are frequently used as high permittivity dielectrics [58, 59]. Alkaline earth titanates such as $CaTiO_3$, $SrTiO_3$ and $BaTiO_3$ etc. have been also studied extensively for technological applications in primary science as well as electronic devices due to its exciting electrical properties, structural behaviour and chemical stability. The high dielectric constant in $BaTiO_3$ ceramics results due to transition in their crystal structure from cubic to tetragonal. In $BaTiO_3$ ceramic, the temperature was a substantial factor which affects the crystal structure and polarization characteristics of $BaTiO_3$ [60]. The $BaTiO_3$ has possessed a spontaneous polarization at room temperature due to the presence of non-centrosymmetry in the centre of oxygen octahedron [61]. As the temperature increases, the thermal vibration in $BaTiO_3$ results in the random orientation of titanium ions to the octahedral interstitial position. The dielectric properties are also enhanced by making the solid solution of two phases like ferroelectric $BaTiO_3$ and non - ferroelectric $BaSnO_3$ in which the replacement of Sn^{4+} ion on the Ti^{4+} site results a shift of Curie temperature. Due to shift in curie temperature, a high dielectric constant value was obtained because of the presence of different conductive regions which produced a chemical microheterogeneity at the level of nano-polar regions (Random occupation of Sn^{4+}, Sn^{2+} at Sn-site and Ti^{4+}, Ti^{2+} at Ti-site) [62].

1.10.2 Magnetic Properties

The perovskites compounds also shows interesting magnetic properties [63, 64]. Among them the $LaMnO_3$ showed versatile magnetic properties at liquid air temperature while the other perovskites like $LaCrO_3$ and $LaFeO_3$ are not [65, 66]. It appeared that $LaMnO_3$ was ferromagnetic at liquid air temperature only when it contains partial fraction of manganese ion like higher valence state as well as lower valence state than Mn^{3+}. The manipulation of valance state is also performed by treating $LaMnO_3$ at high temperature in presence of oxygen rich atmosphere. In this process, the formation of oxygen vacancy takes place in sample and electron associated with oxygen vacancy compensate the overall charge neutrality which can be used in manipulation of the valence state of Mn. The partial substitution of alkaline earth element at La site and higher valence atom at Mn-site like $La^{3+}Mn^{3+}O_3^{2-}$ - $Me^{2+}Mn^{4+}O_3^{2-}$ (Me^{2+} larger divalent ions) is another manipulative method [67]. These methodology is tried for investigating the binary system such as $LaMnO_3$-$CaMnO_3$, $LaMnO_3$-$SrMnO_3$, $LaMnO_3$-$BaMnO_3$, $LaMnO_3$-$CdMnO_3$, $LaMnO_3$-$PbMnO_3$ [66, 68]. In all these systems, at least over a certain compositions, ferromagnetic mixed crystal was formed. The ferromagnetism of hole doped specimen is explained by double exchange interaction taking place between Mn^{3+} and Mn^{4+} ions [66, 68]. The magnetic properties can be modified in non-magnetic perovskites by incorporating small amount of magnetic ion or rare earth elements also known as dilute magnetic semiconductor (DMS) [67]. The various rare earth doped ion into BaTiO3, $BaSnO_3$, $LaMnO_3$, $LaAlO_3$ etc. have been widely investigated for spintronic applications [69, 67]. In case of rare earth element doping, the magnetism can be explained in terms of direct interaction, exchange interaction and bound magnetic polaron (BMP) model [70, 71].

1.10.3 Optical Properties

The invention of a white light emitting diode (LED) has brought revolution to this century's lighting technology that suppressed the conventional use of incandescent or

fluorescent lamps. They have excellent properties such as high brightness, cost reliable, low power consumption and long service life [72, 73]. Rare earth (RE) doped phosphors material have found important applications in the development of white LEDs [74]. The perovskite structure ($A^{2+}B^{4+}O^{2-}$) doped with activators (Er^{3+}, Yb^{3+}) have become significant importance because of their easily tunability of emission properties found in different regions [75]. These perovskite oxides form very stable matrices both chemically/physically and also capable to work in different environments. Particularly, in the field of solid state lighting these oxides based phosphors become a potential candidate in the area of field emission display (FEDs) and plasma panel display (PDPs) devices [76]. The luminescence properties of perovskite oxide based phosphors having structure such as $A^{2+}B^{4+}O^{2-}$ (A: Ca, Sr, Ba and B: Sn, Ti, Zr, Si, Hf, etc.) activated with different rare earth ions including Sm^{3+}, Tm^{3+}, Pr^{3+}, Eu^{3+}, Tb^{3+}. The orange, red, green, yellow and red-orange emissions were extensively studied [77, 78].

Recently, the transparent and conductive oxides (TCO) with the perovskite structure were explored extensively by ionic substitution and carrier doping. The thin films of In, Sb, La-doped $SrTiO_3$, Nb-doped $CaTiO_3$, and Cd_3TeO_6 have been extensively studied for TCO application [79]. The thin film of La and Sb-doped $BaSnO_3$ deposited on the substrate of $SrTiO_3$ (001) (STO) using laser ablation method are found that these films show not only the good stability but also high conductivity and good optical transparency in the visible region. Moreover, the growth parameters for these films are compatible with the films of other perovskite such as ferroelectric (Pb, Zr)TiO_3. The TCO films of these materials can be used as a potential candidate for optoelectronic device applications especially based on perovskite heterostructures [80].

1.11 Applications of Perovskites

Thus one can conclude that the perovskite type structures are the most stable structure. The perovskites are studied extensively and tried for various kinds of application dependent on

the modification in perovskite oxides. The undoped /rare earth or transition metal modified $LnMnO_3$ perovskites are found as a potential candidate in the application of electrolyte [81], cathode and anode materials for solid oxide fuel cell [82]. $A^{2+}B^{4+}O_3^{2-}$ type perovskites structure are used for sensor applications to senses different gas like ethanol, hydrogen, oxygen, nitrogen, ammonia etc. [83]. The modified perovskite type structures $AA'BB'O_{3-\delta}$ (A = Ln Lanthanides, A' = Alkaline earth metal, B = Transition metal/Alkali metal B' = Rare earth element, those have valance state other than cation B) have been used in application of electronic ceramics [84], superconductors [85], and solid state lighting [86]. Alkaline earth elements based titanates ($BaTiO_3$) is extensively used as ferroelectric as well as piezoelectric materials due to their tetragonal crystal structure. Further modification made by rare earth element and transition metal in $BaTiO_3$, it can be used in spintronics and phosphor application for imaging purposes [87, 88]. However, rare earth modified $SrTiO_3$ was used as electrode materials (Cathode/anode) in solid oxide fuel cell, Sm^{3+} modification gives better luminescence in the intense emission in orange region and Eu^{3+} modification results intense red orange emission [89]. Although, the alkaline earth stannates ($BaSnO_3$) is found as a wide band gap semiconductor at room temperature and modification by rare earth and transition metal it can be used for electrode materials in solid oxide fuel cell (SOFC), electrode material for Dye Sensitized Solar Cell [90], dilute magnetic semiconductor (DMS) [67], magnetic memory devices [91]. Even though it can be further transforms to conductor by changing the processing parameters and doping concentration [92]. The perovskite not only in individuals but also their solid solution can be used in dielectric chip, thermal stable capacitor, barrier layer capacitor, memory devices and so on [90, 93].

Hence, it can be concluded that it can be used in multiple applications based on variation in processing parameters, change in doping and their concentrations, structural transitions and charge compensation mechanism.

1.12 Protonic conducting oxides: principle and defect chemistry

Protonic conducting oxides can be considered as electrolytes in which hydrogen ions are the major charge carriers. Protons, usually, are not part of the component of oxides. The requirements for the introduction of protonic defects into an oxide-based proton conductor can be simply stated as [94]: **(1)** It possesses an oxygen deficient lattice, either structurally, or via acceptor doping **(2)** It can incorporate water at modest applied vapor pressures, *i.e.* < 1 atm **(3)** It permits the rapid transport of protons once these have been formed.

1.12.1 Proton defect formation

For large band gap perovskite (ABO_3) oxides, proton conduction almost exclusively involves acceptor-doped systems with charge-compensating oxygen vacancies in the dry state. When it is exposed to humidified atmosphere, the oxygen vacancies are replaced by hydroxyl groups which means that protons are incorporated into perovskite structure as shown in **Figure 1.7**. Protons are located in the crystal lattice close to oxide ions due to electrostatics attraction and can rotate & migrate between adjacent anions with so called Grotthuss mechanism [95] which is the basis of proton conduction and the defect reactions are expressed in Kröger-Vink notation as following:

$$2B_B^{\times} + O_O^{\times} + M_2O_3(s) \xrightarrow{yields} 2M_B' + V_O^{\cdot\cdot} + 2BO_2(s) \quad (1.14)$$

$$H_2O(g) + V_O^{\cdot\cdot} + O_O^{\times} \overset{yield}{\Longleftrightarrow} 2OH_O^{\cdot} \quad (1.15)$$

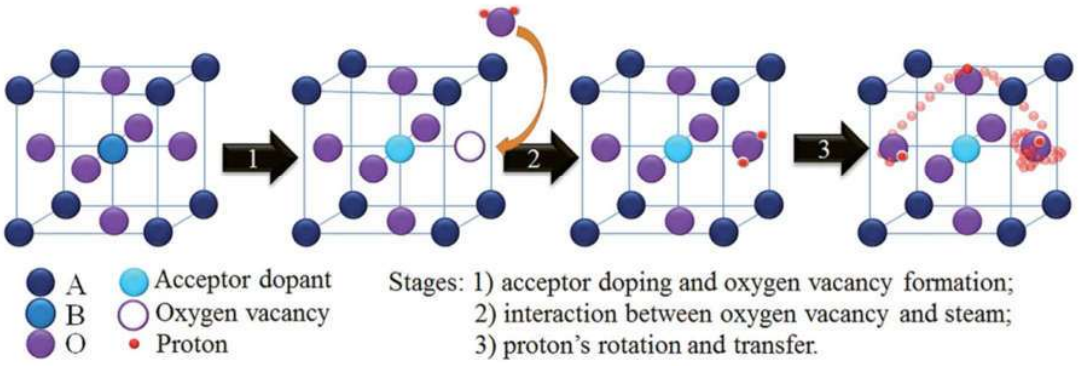

Figure 1.7 Formation of proton and migration mechanism in the ABO_3 perovskite structure.

However, it is well known that non-stoichiometry, atmosphere, dopant nature *etc.,* greatly influence defect reaction and transport properties of proton conductors. For instance, for the typical proton conductors, *i.e.* strontium cerate, barium cerate and barium zirconate, it has been reported that BaO evaporates easily from the surface of sintered pellets due to high sintering temperature [96], and some analysis also indicates the possible existence of an amorphous Ba-rich phase at grain boundaries [97]. Barium oxide deficiency may result in the trivalent ion residing on Ba-site. For instance, microanalysis of Nd-$BaCeO_3$ solid solutions indicated that the solutions could be represented by a general formula $Ba_{1-x}Nd_xCe_{1-y}Nd_yO_{3-(y-x)/2}$ $(V_{\ddot{O}})_{(y-x)/2}$ in which Nd is partioned on both Ba and Ce sites [98.]. The existence of Ba^{2+}-site occupation has also been proposed by theoretical calculations for dopants such as La, Nd and Sm in doped $BaCeO_3$ [99.].

$$2Ba_{Ba}^{\times} + M_2O_3 + V_O^{\cdot\cdot} \rightarrow 2M_{Ba}^{\cdot} + O_O^{\times} + 2BaO \qquad (1.16)$$

This reaction consumes oxygen vacancy instead of creating new vacancies and thus might lower the protonic conductivity.

1.12.2 Hydration thermodynamics of acceptor-doped perovskite oxides

As mentioned above, when the doped perovskite oxide with oxygen vacancies is exposed to water atmosphere, oxygen vacancies are filled by hydroxyl ions as described **Eq. (1.14-1.15)**. The thermodynamics associated to **Eq. (1.14-1.15)** is an important parameter for describing proton conduction, which can evaluate the dissolution and concentration of protons in the materials. The hydration thermodynamics of such reaction might be determined theoretically or experimentally basing on semi-empirical calculation and first principles calculations or thermogravimetric and conduction data.

1.12.2.1 Theoretical calculations

The enthalpy of water incorporation has been calculated by semi-empirical calculation for typical proton conductors such as $BaCeO_3$, $SrZrO_3$ and $CaZrO_3$ compounds [99, 100]. Based on in **Eq. (1-2)**. The enthalpy of water dissolution (proton incorporation), E_{H2O} can be calculated using the following equation [99, 100]:

$$E_{H_2O} = 2E(OH_O^{\cdot}) - E(V_O^{\cdot\cdot}) + E(PT) \quad (1.17)$$

Where, $E(OH_O^{\cdot})$ is the energy associated with substitution of O^{2-} with an OH^- group, $E(V_O^{\cdot\cdot})$ the energy needed to create an isolated oxygen vacancy and $E(PT)$ is the energy of proton exchange reaction at the surface which hydroxide ions replace lattice oxygen ions: $O^{2-} + H_2O(g) = 2OH^-$. It is independent of the crystal structure, calculated to be -11.77 eV [100, 101].

The results calculated based on **Eq. (1.17)** indicate negative dissolution enthalpy, which signifies probable dominating proton conductivity at low temperature in these materials which is consistent with the experimental conclusions. Of course, uncertainties in the absolute calculated values are important due to the limits of the very simplistic

model employed. Nevertheless, there is reasonable quantitative accord with the few available experimental values [102].

Recently, the hydration energies of barium zirconate and barium stannate doped by various trivalent elements (Gd^{3+}, In^{3+}, Nd^{3+}, Sc^{3+} and Y^{3+}) have been also calculated from first principles calculations with an "isolated defects" model as well as with a model considering the interaction energies between the dopants and oxygen vacancies/protons [103, 104]. The authors deduced hydration energies within the framework of various models, and estimated the hydration Gibbs free energy by accounting for vibrational energetic and entropic effects. In the case of Y-doped $BaSnO_3$, the hydration energy (12.5 mol % Y doping) calculated is - 0.69 eV. The experimental enthalpy of 10 mol % Y-doped $BaSnO_3$is - 0.62 eV, for 25 mol % of Y content it is - 0.83 eV, and for 50 mol % of Y content -1.05 eV [20]. The results of computation are good agreement with the experimental results.

Unfortunately, the theoretical calculations are unable to evaluate the value of the hydration reaction entropy leading thus to some important uncertainty for the real temperature range of a material to work as a proton conductor.

1.12.2.2 Experimental access to hydration thermodynamics

To analyse hydration thermodynamics, the equilibrium expression for **Eq. (1.15)** between oxygen vacancies and water vapour to form protons is [105]:

$$K = \exp\left(\frac{\Delta S^{\circ}}{R}\right)\exp\left(-\frac{\Delta H^{\circ}}{RT}\right) = [OH_O^{\cdot}]^2/([V_O^{\cdot\cdot}][O_O^{\times}]P_{H_2O}) \quad (1.18)$$

Where, the square brackets denote molar fractions or volume concentrations (but in general not site fractions).

The electroneutral condition of acceptor-doped oxide with oxygen vacancies and protons is:

$$2[V_O^{\cdot\cdot}] + [OH_O^{\cdot}] = Acc' = constant \quad (1.19)$$

Where *Acc* denotes acceptors in general. The approximation is made here that the concentration of holes/electrons is negligible. If defect concentrations are small, we could assume that $[O_O^{\times}]$ equals the concentration of oxide ion sites, $[O_O^{\times}] + [V_O^{\cdot\cdot}] + [OH_O^{\cdot}] = [O]$. In molar concentration, for perovskites oxides, $[O] = 3$ then:

$$K = \frac{4[OH_O^{\cdot}]^2}{P_{H_2O}(Acc' - [OH_O^{\cdot}])(6 - [Acc'] - [OH_O^{\cdot}])} \tag{1.20}$$

And the concentration of protonic defects as a function of P_{H_2O} and K is:

$$[OH_O^{\cdot}] = \frac{3Kp_{H_2O} - \sqrt{Kp_{H_2O}(9Kp_{H_2O} - 6Kp_{H_2O}[Acc'] + Kp_{H_2O}[Acc']^2 + Kp_{H_2O} + 24[Acc'] - 4[Acc']^2)}}{Kp_{H_2O} - 4} \tag{1.21}$$

Because the formation of protonic defects according to **Eq. (1.15)** is accompanied by a significant weight increase, the concentration of protonic defects as a function of temperature and water partial pressure is usually measured by thermogravimetric analysis (TGA), or indirectly by conductivity measurements. The fitting of experimental data to the model described above provides the equilibrium constant K and K vs temperature is well described by **Eq. (1.18)** corresponding to an Arrhenius type behavior for $K(T)$, giving standard hydration enthalpies and entropies (ΔH° and ΔS°) [15].

Hydration thermodynamic parameters are important in that they determine whether at a given temperature the material is primarily dominated by oxygen vacancies or protons [17]. The enthalpy of hydration (**Eq.1.15**) varies considerably with some apparent correlation to materials properties.

Norby *et al*. [105] reported that the enthalpy of hydration for rare earth sesquioxides becomes more negative as the oxide gets more stable *i.e.* as the enthalpy of formation gets more negative, the stable Y_2O_3, Er_2O_3 and Yb_2O_3 thus contain protons up to very high temperatures

while less stable La_2O_3 dehydrates even at very moderate temperatures. However, the mobility of protons decreases as their stability in the oxide increases, the highest proton conductivity being thus obtained as a compromise in the middle of the series for Gd_2O_3.

In perovskite-related oxides, Kreuer *et al.* [15] suggested that the enthalpy of hydration reaction tends to become more negative with decreasing electronegativity of cations interacting with the lattice oxygen *i.e.* with decreasing Bronsted basicity of the oxide. Norby *et al.* [105] have developed a correlation between the hydration enthalpy and the difference ΔX_{B-A}in electronegativity between the cations populating the B-site and the A-site of the perovskite. **Figure 1.8** shows precisely an update of this correlation plot [17]. A linear trend from the enthalpies can be presented roughly.

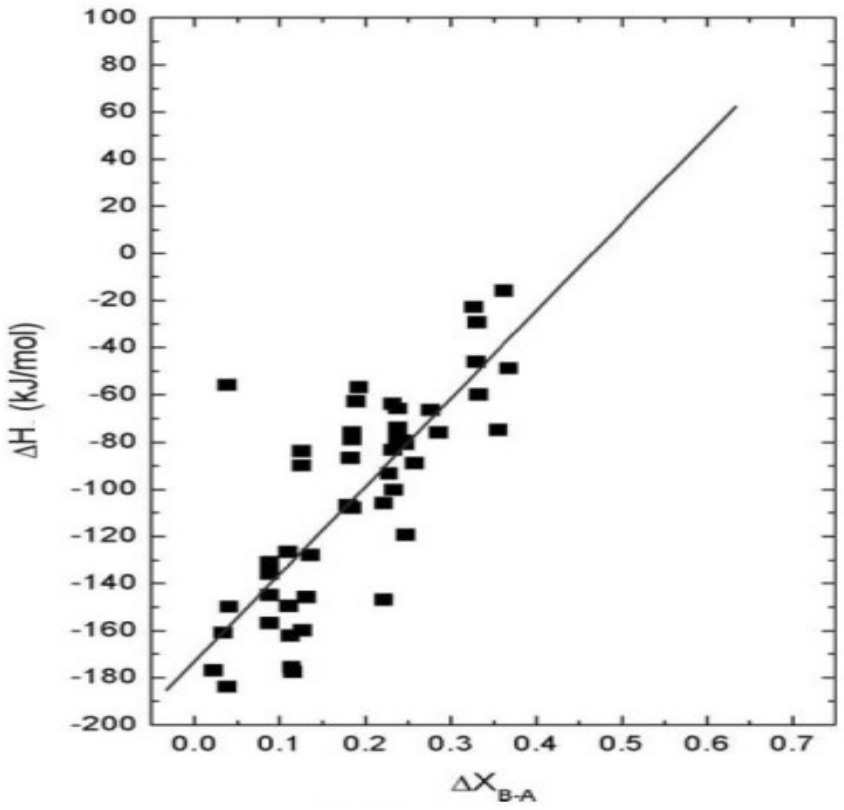

Figure 1.8 Hydration enthalpy vs difference in Rochow-Allred electronegativities between B- and A-site constituents in perovskites [17].

The standard entropy change ΔS° appears to end up around -120 J/mol•K, as expected empirically for the loss of 1 mol of gas [105]. Nevertheless, some perovskites such as $BaCeO_3$ have large negative values (exothermic) of more than -150 J/mol and they are thus dominated by protons in wet atmospheres and suppose a high temperature to shift the equilibrium to the left. Others, such as $SrTiO_3$ have moderate negative entropies and are dominated by protons only at relatively low temperatures [17].

1.12.3 Proton transport

It is well known that proton transport includes transport of protons (H^+) and any assembly that carriers protons (H_3O^+, NH_4^+, OH^- et al.). There are two principal mechanisms well recognized to describe the transport of proton: the vehicle mechanism and the Grotthuss mechanism [11, 15, 106, 107].

For the vehicle mechanism, the proton moves together with a "Vehicle" as passenger on a large ion (H_3O^+, NH_4^+, OH^- et al.). This mechanism is mainly observed in aqueous solution, other liquids/metal and compounds with loose bonded small molecules which is usually restricted to materials with open structures (i.e. channels, layers) to allow the passage for the large ions and molecules.

The other mechanism is the so-called Grotthuss mechanism. This was proposed to explain the high diffusivity of H^+ ions in water and involves the protons tunnelling from one water molecule to the next via hydrogen bonding. This mechanism is thought to be at the origin of the high proton mobility in solid acid salts and proton conducting oxides. Actually, quantum MD simulations revealed the details of a typical Grotthuss mechanism in proton conducting perovskite oxides [102, 107, 108]. The protons always residing on oxide host ions exhibit thermal rotation and stretching vibrations. The principal features of the

proton diffusion process are the rotational diffusion of the proton to set up the hydrogen bonds OH-O between the two oxide ions, the decrease of their distance and the proton transfer towards the adjacent oxygen ion via stretching vibration. The rotational motion of the proton in the O-H group is rapid which allows the reorientation of the proton towards the next oxygen ion before the transfer process. The transfer process was calculated to be the rate-limiting step in the considered perovskites. A typical proton diffusion trace as obtained from MD calculations is shown in **Figure1.9** [109].

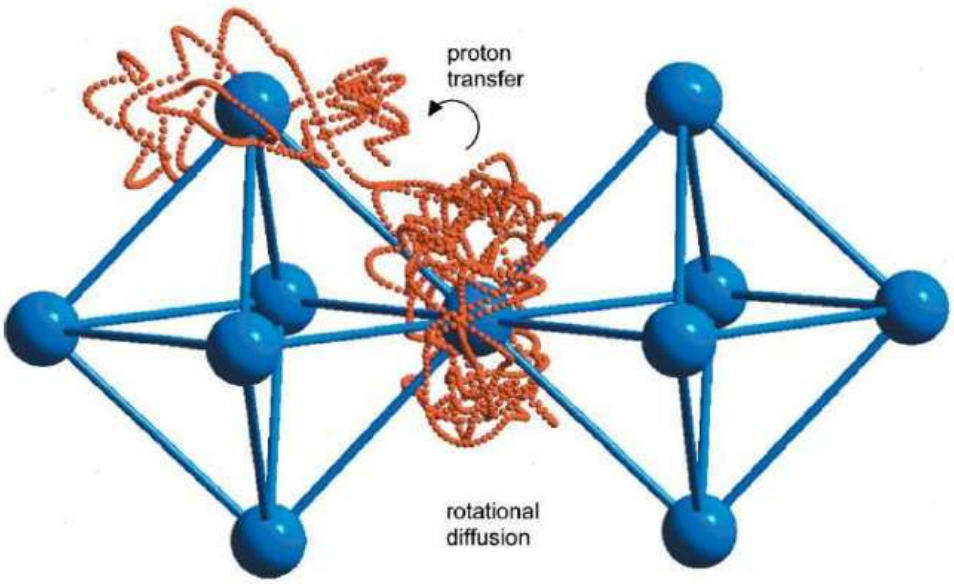

Figure 1.9 The trace of a proton in a perovskite showing the two principal features of proton transport: rotational diffusion and proton transfer [109].

1.12.4 Effects of defect-dopant association

The mutual association of the proton defects, oxide ions and metal cations in the proton conducting oxides comprises not only hydrogen bonding but also stronger covalent and ionic interactions [107]. For instance, the association between oxygen vacancies

and acceptor dopants has been reported to explain the non-Arrhenius behaviour of oxygen ion conduction in acceptor-doped oxides such as zirconia, ceria, lanthanum gallate and others [105]. Oxygen vacancies associated to acceptor dopants can be written:

$$V_O^{\cdot\cdot} + Acc' = (V_O^{\cdot\cdot}Acc)^{\cdot} \quad (1.22)$$

If the oxygen vacancies are trapped as associates, it will also influence the hydration thermodynamics. The hydration of the associate will be written [17.]:

$$H_2O(g) + (V_O^{\cdot\cdot}Acc)^{\cdot} + O_O^{\times} = 2[OH_O^{\cdot}] + Acc' \quad (1.23)$$

The oxygen vacancies are stabilized and the hydration enthalpy perhaps can be expected to be less favourable than that of the free vacancies, provided that the protons dissolved are less associated to the acceptor [17, 105].

Similar association between proton and the dopant might also act in the opposite direction favouring a higher proton concentration but giving a smaller mobility. Proton will tend to be trapped by acceptors according to this equation [17].

$$OH_O^{\cdot} + Acc' = (OH_OAcc)^{\times} \quad (1.24)$$

Kreuer *et al.* [110.] found that $BaZrO_3$ doped with Y exhibits a lower activation energy and higher conductivity than with the same amount of Sc while the hydration enthalpy of $BaZrO_3$ doped with Sc (-119.4 kJ/mole) is much more negative than with Y (-79.5 kJ/mole). They attributed this to oxide ions coordinated to Sc becoming more electron rich (basic), thus bonding protons more strongly. Islam *et al.* [111] also predicted that the lowest binding energy of hydroxyl-dopants is for Y and the strongest association is for Sc for $BaZrO_3$ as calculated by atomistic simulation which is in agreement with Kreuer's results. All in all, it appears that there are effects of dopants but trapping leading to associates is hardly evidenced experimentally in conductivity measurements so far [17].

1.12.5 Isotope effect

Isotope effect is a major tool to confirm the protonic nature of conductivity in solid oxide conductors. The study of the isotope effect most often involves substitution of D for H. This produces a mass change by a factor of 2 which is far greater than that available from isotopes of other elements. Different theories have been developed to understand the mechanism of isotope effect such as classical theory, semi-classical theory and tunnelling theory [112-115].

The classical theory is adopted first to describe the isotope effect due to influence of the pre-exponential term of conductivity. The proton (or deuteron) "hops" from one lattice site to another over a potential energy barrier as depicted in **Figure 1.10**, as a function of the configurational coordinate [116].

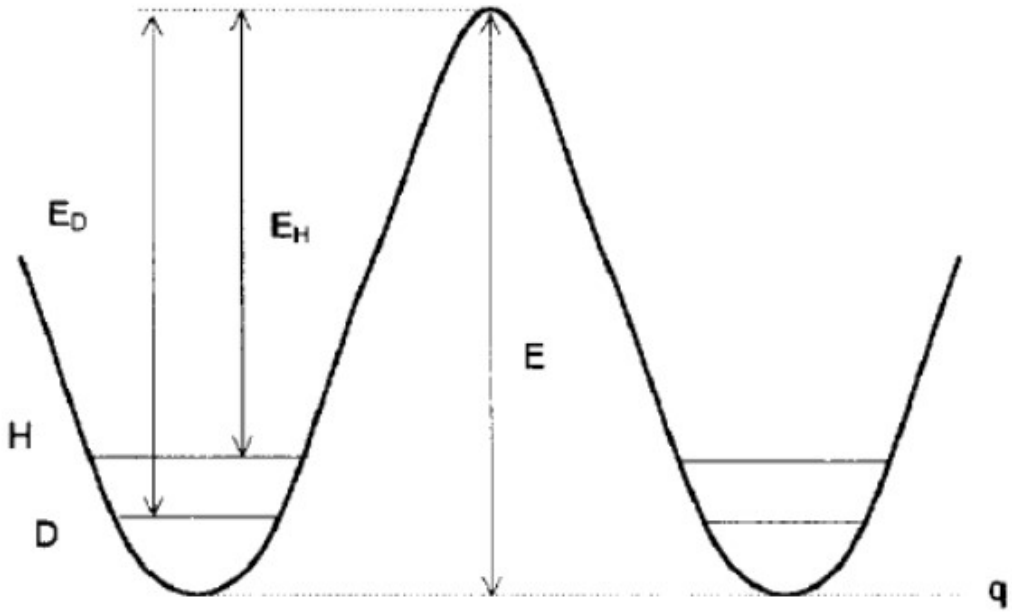

Figure 1.10 Schematic diagram of potential barrier for a proton (or deuteron) transfer reaction as a function of the configurational coordinate of the hopping atom [112.]

For an ionic conductor, the conductivity has an Arrhenius form described by:

$$\sigma = \frac{A}{T}\exp\left(-\frac{E_a}{KT}\right) \tag{1.25}$$

Where A is pre-exponential term, T is the absolute temperature, k is Boltzmann constant and E_a is the activation energy. More specially, the pre-exponential term is described by:

$$A = \frac{Zq^2\lambda^2\omega_o C_o}{6Vk} \tag{1.26}$$

Where z is the number of directions in which the conductivity jump may take place, q is the charge of hopping ion, λ is the jump distance, C_o is the charge of hopping ion, V is the volume of unit cell, k is Boltzmann constant, ω_o is the frequency factor, described by:

$$\omega_o = \nu_o exp\left(\frac{\Delta S}{k}\right) \tag{1.27}$$

Where ΔS is the vibrational entropy, ν_o is an appropriate 'attempt frequency' which for a light atom, involves an effective mass that falls close to the mass of the hopping atom. In the case where ν_o is only the OH stretching frequency, a harmonic oscillator model is used which yields the relationship $\nu_o \propto 1/\sqrt{m}$ where m is the effective mass.

Hence, the conductivity can be written as:

$$\sigma = \frac{A}{T}\exp\left(-\frac{E_a}{KT}\right) \propto \frac{1}{\sqrt{m}}\exp\left(-\frac{E_a}{KT}\right) \tag{1.28}$$

Thus, in the classical theory, the activation energy is independent of the isotope, and the effective mass is the only parameter that affects the conductivity. The heavier mass of deuteron compared with hydrogen leads to a lower conductivity which contributes to the observable isotope effect.

However experimentally, the activation energy is in most cases different for hydrogen and deuteron with $E_D > E_H$ as explained by **Figure 1.10**. This suggests that the activation energy E_a looks some contributions from the isotope effect. Semi-classical

theory which takes the zero-energy difference into consideration, is adopted here. If the activated state is independent of the isotopic mass, we can expect for the activation energy difference:

$$E_D - E_H = \frac{1}{2}h(\nu_H - \nu_D) \quad (1.29)$$

For the OH ions in the perovskite oxides, the OH stretching frequency ν_H is close to 10^{14} s^{-1} [35] and with $\nu_D/\nu_H = 1/\sqrt{2}$, we get $E_D - E_H \cong 0.055\ eV$.

If the proton is dominating charge carriers, the isotope effect will be clearly observable first from conductivities values thereafter from activation energies. Otherwise it can be concluded that the conductivity mechanism is not protonic.

In practice both classical and non- classical isotope effects are encountered. For example with $SrZr_{0.94}Y_{0.06}O_{2.97}$, Huang *et al.*[117] observed a classical isotope effect of 2 from 150 to 500 °C but this disappeared at higher temperatures where electronic conductivity becomes dominant while Scherban *et al.* [118] reported that σ_H/σ_D is close to 2.5 in 5 mol % Yb-doped $SrCeO_3$ compound at room temperature and concluded that protonic hopping follows a non-classical behavior. Initially, tunnelling was suggested to explain how protons could overcome the strong bond to their host oxygen ions and enhance proton diffusion at low temperature. However tunnelling was abandoned as the experimental evidence for the large isotope effects was proven wrong [112] and proton migration could be described by use of oxygen ion dynamics [105].

1.12.6 Mixed conductivity in proton conductors

We only consider ionic species as compensating charges in response to doping until now. Nevertheless, it is widely accepted and reported that the electrical properties of perovskite-type protonic conductors at temperatures above 700 °C are often characterised of course by oxygen ion conductivity but also by n- or p-type conductivity [119,

120]. The relationship between the oxygen ion, n- and p-type electronic conductivities and oxygen partial pressure in acceptor-doped perovskite compounds is presented in this section based on defect chemistry.

When trivalent dopants are incorporated into perovskite oxides, oxygen ion vacancies ($V_O^{\cdot\cdot}$) are created to maintain charge neutrality. In oxygen rich atmosphere, the oxygen vacancies tend to react with gaseous oxygen to produced electron holes:

$$\frac{1}{2}O_2(g) + V_O^{\cdot\cdot} \overset{yield}{\Longleftrightarrow} O_O^{\times} + 2h^{\cdot} \tag{1.30}$$

At low oxygen partial pressure, on the opposite, the oxygen ion can leave their sub-lattice generating oxygen ion vacancies ($V_O^{\cdot\cdot}$) and electrons$(e)'$:

$$O_O^{\times} \overset{yield}{\Longleftrightarrow} \frac{1}{2}O_2(g) + V_O^{\cdot\cdot} + 2e' \tag{1.31}$$

In hydrogen free atmosphere and low water pressure, the electro neutrality equation, is given by:

$$2[V_O^{\cdot\cdot}] + p \overset{yield}{\Longleftrightarrow} [M_B'] + n \tag{1.32}$$

There are three different Brouwer-type charge neutrality condition $(e', V_O^{\cdot\cdot}), ([M_B'], V_O^{\cdot\cdot}), ([M_B'], h^{\cdot})$ from low to high oxygen partial pressure [121]. However for mostly proton conductor with high oxygen concentration formed by acceptor-dopant perovskite oxides, $[M_B'] \gg p, n$ with the concentration of oxygen vacancies fixed by [122]:

$$2[V_O^{\cdot\cdot}] = [M_B'] = Constant \tag{1.33}$$

Combining **Eqns. (1.30)-(1.33)**, the concentration of different charge carriers can be given by:

$$p = h^{\cdot} = 2^{-\frac{1}{2}} K_{ox}^{\frac{1}{2}} [M_B']^{\frac{1}{2}} P_{O_2}^{\frac{1}{4}} \tag{1.34}$$

$$n = e' = 2^{-\frac{1}{2}} K_{red}^{\frac{1}{2}} [M_B']^{-\frac{1}{2}} P_{O_2}^{-\frac{1}{4}} \tag{1.35}$$

Where K_{ox} and K_{red} are the equilibrium constant of **Eq. (1.30)** and (1.31), $p, n, [M_B']$ are the concentrations of the holes, electrons and dopants, p_{O_2} is the oxygen partial pressure.

The effective charge carriers consist then of oxygen vacancFies, electrons and holes, which lead to oxygen ion, electronic and hole conductivity respectively. The conductivity of mixed conductors is explained as

$$\sigma_T = \sum \sigma_i = \sum q_i C_i B_i \tag{1.36}$$

Where, σ_i is the conductivity component contributed by charge carrier species i, C_i is the concentration of the charge carrier, q_i is the charge and B_i is the mobility of charge carrier species i. In most cases, the component C_i is the parameter that is modified by controlled atmosphere and chemical composition while the mobility B_i is essentially affected by temperature.

Combining **Eqns. (1.34)-(1.36)**, the conductivity of mixed conductor also can be explained as [43]:

$$\sigma_T = A + B{p_{O_2}}^{-\frac{1}{4}} + C{p_{O_2}}^{\frac{1}{4}} \tag{1.37}$$

Where the first term (A) is the p_{O_2} independent oxygen ion conductivity, the second and the third terms are the contributions from electrons and electron holes respectively. Given the total conductivities in different oxygen pressures at different temperatures, we can use **Eq. (1.37)** to fit the data and deconvolute and determine the ionic, *p*- and *n*-type conductivities as a function of temperature and oxygen partial pressure.

For proton conductor, we should also take into account proton defects at high water vapor pressure. When increasing oxygen partial pressure from low oxygen partial pressure, three different charge neutrality conditions have to be considered *i.e.* the major defect pairs are changed sequentially from $(e', OH_O^{\cdot})$ to $([M_B'], OH_O^{\cdot})$, $([M_B'], h^{\cdot})$ [121]. The dominant ionic defect shifts from $V_O^{\cdot\cdot}$ to $OH_O^{\cdot}$ as P(H2O) increases at immediate oxygen pressure. In order to avoid a situation into which we have at the same time oxygen

vacancies, holes and protons, we investigated the effect of dopants nature and contents on transport properties in an atmosphere (Argon) at which oxygen vacancies were measured to be the main charge carrier in dry atmosphere. It is clear that at intermediate temperature in air which is actually the atmosphere encountered at cathode side in fuel cells, the coexistence of holes and protons beside that of oxygen vacancies should be considered.

1.13 Proton conducting oxides: Materials

1.13.1 Proton conductivity in acceptor-doped peroskite oxides

Perovskite oxides offer in almost all respect in a wide variety of properties because of the structure ability to host varying cations, substitutions, non-stoichiometry and defects of many kinds. Proton conductivity is found in a range of perovskites oxides, ABO_3. Perovskite-type oxides have the general formula $A^{2+}B^{4+}O_3$, where A can be group IIA element or transition metal in the +2 oxidation state and B is a transition metal, Ce, Zr, Sn, Ti in the +4 oxidation state. The structure of perovskites-type oxide (i.e.$SrCeO_3$) is explained in **Figure 1.11**. In the orthorhombic perovskite structure, A ions occupy the corners of the elementary cell, the B ions the volume center and O^{2-} ions the surface center. In this structure, the larger A^{2+} and the O^{2-} ions build a orthorhombic densest ball packing together and a quarter of the octahedral holes is filled with small B^{4+} ions. Each A^{2+} ion is coordinated with 12 O^{2-} ions, each O^{2-} ion is surrounded by four A^{2+} ions and two B^{4+} ions. The octahedrons of (BO_6) are linked by sharing corners structure can distort and deform under definite conditions so that the structure symmetry degree is lowered. **Figure 1.12** show the partial proton conductivity for a number of acceptor-doped perovskites, calculated from data for proton mobility and thermodynamic of hydration [17].

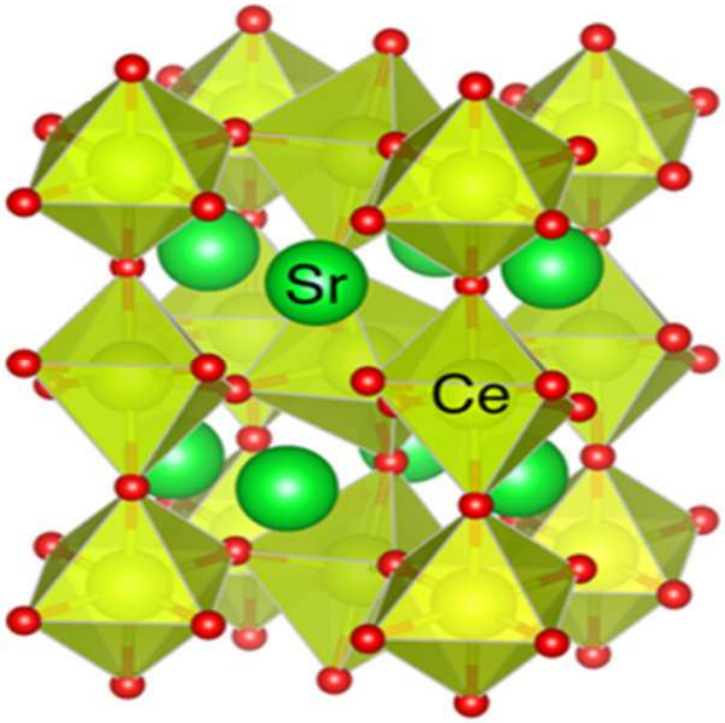

Figure 1.11 Perovskite structure of $SrCeO_3$

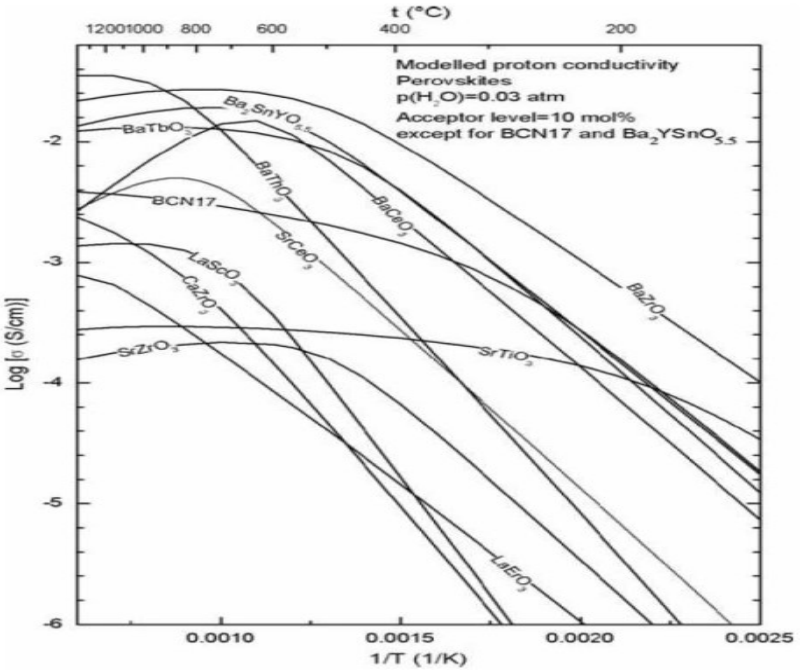

Figure 1.12 Partial proton conductivity vs. 1/T for bulk of selected perovkites at $P(H_2O) = 0.03$ atm, calculated on basis of proton mobility and hydration thermodynamics parameters [17]**.**

Among II-IV perovskites ($A^{2+}B^{4+}O_3$), a recent analysis of available data provided the following guidelines for the composition of perovskite with high proton conductivity and good thermodynamics stability [123]: (a) Except for the stability with acidic gases, which is almost independent of the choice of the A-cation, all relevant properties are superior for an A-site occupation by barium compared to other alkaline earth ions. (b) However the choice of B-cation requires some compromise. The B-cations should be of medium size with an amphoteric nature and should form no significant covalent bonds with oxygen ligands. Small B-cations lead to high packing densities and reduce the water solubility while large B-cations reduce the thermodynamics stability. It is well known that cerates and zirconates show large negative hydration enthalpies and small activation energies for proton migration. Among these materials, Gd-substituted $BaCeO_3$ shows the highest protonic conductivity *i.e.* ~ 0.05 $S \cdot cm^{-1}$ at 600 °C, temperature at which protons are the main charge carriers [124, 125]. This makes barium cerate considered as a potential candidate for fuel cell electrolyte. However, its long-term stability remains a concern in the presence of CO_2 and water-containing atmosphere [124, 126]. $BaCeO_3$ and $SrCeO_3$ react with CO_2 to form carbonates and form alkaline earth hydroxides at high water activities. Indeed, this excludes the use of any hydrocarbons from being used as fuels because this inevitably leads to the production of some CO_2 and H_2O. The stability of cerates can be increased by chemical modifications *i.e.* by partially replacing Ce by Zr ($\geq$ 0.4), although the proton conductivity will decrease with increasing Zr content [127, 128]. The developments of these materials require thus to find a compromise between conductivity and stability characteristics.

Zirconates [129, 130] in particular Y-doped $BaZrO_3$ combine high bulk proton conductivity with high thermodynamics stability (they are stable in acidic media and CO_2). At

low temperature (< 700 °C) under wet atmosphere, the bulk conductivity of Y-doped $BaZrO_3$ is even slightly higher than the proton conductivity of BaCeO3-based oxides [15] and is considered to be a good candidate electrolyte material in the intermediate temperature range. However low sinterability and high grain boundary impedance are two major problems which is unfavourable to make these materials commercial. If these problems are solved BaZrO3 can be an excellent electrolyte material for intermediate temperature fuel cells [131]

Other ABO_3 perovskites such as praseodymiates [132, 133.], hafnate [134], thorates and terbates [135] (B site occupied by Pr, Hf, Th and Tb, respectively) were also studied as new proton conducting materials. They readily incorporate some protons at intermediate temperature but their conductivity is limited or in part due to hole contribution.

Among III-III perovskites ($A^{3+}B^{3+}O_3$), La^{3+} is the only common A-site cation, B is Sc^{3+}, Y^{3+}, In^{3+}, Er^{3+} et al. [136-142]. Of these, $LaScO_3$ hydrates well but exhibits medium proton mobility and a proton conductivity peaking just above 10^{-3} S/cm. $LaYO_3$ and $LaErO_3$ are also perovskite related but with lower tolerance factors and lower conductivity.

'Complex perovskites' represent another family of compounds and usually suppose two B-site cations of different valence, typically in simple ratio to form a certain valence sums. Nowick and coworkers introduced this new class of complex perovskites as oxide ion and proton conductors in which the B-site cation ordering is essential [143-145.]. These complex perovskites have the general formula $A_2(B'_{1+x}B''_{1-x})O_{6-\delta}$ and $A_3(B'_{1+x}B''_{2-x})O_{9-\delta}$ both of which have two different ions occupying B-sites. In both cases, the A ions is charged 2+, in the former compound B' is 3+ and B" is 5+ while in the later, B' is 2+ and B" is 5+ respectively. Thus, the average charge on the B-site is 4+ in both cases. By changing the radio of B' to B" ions, oxygen vacancies can be formed intrinsically and can thereafter induce proton defects under wet atmosphere e.g. $Ba_3(Ca'_{1+x}Nb''_{2-x})O_{9-\delta}$ or

$Sr_3(Ca'_{1+x}Nb''_{2-x})O_{9-\delta}$ [143.]. They were found to combine both good chemical stability and high conductivity.

1.13.2 Proton conductivity in non-peroskite oxide and phosphates

Proton conduction also observed for many non-perovskite classes of oxides, comprising fluorite-related structures and structures with oxide ion tetrahedral. Among the fluorite-related oxides, the MO_2 oxides (M = Zr, Hf and Ce) show very little bulk solubility of protons [17] and the acceptor-doped oxides remain pure oxide ion conductors with negligible proton conductivity at all temperatures.

Proton conductivity in acceptor doped and undoped Ln_6WO_{12} (La, Nd, Gd and Er) has recently been examined. The structure of the tungstate can be explained as an ordered defective fluorite or a disordered pyrochlore [146, 147]. Undoped La_6WO_{12} exhibits proton conductivity peaking at 5×10^{-3} S/cm in wet hydrogen at 900°C [148]. The major disadvantage with the rare-earth tungstates with respect to applications is the chemical stability. Reaction with C-containing species may affect the tungstates, since the formation of WC_x is very stable. The volality of WO_x is another problem, in particular during the fabrication. Some others acceptor-doped pyrochlores, *i.e.* $La_2Zr_2O_7$ show quite high and pure proton conductivity in wet atmospheres [149.].

Proton conductivity in rare-earth sesquioxides were systematically studied within the framework of a consistent description of their defect chemistry by Norby et al. [150-152.]. Sesquioxides are more stable in CO_2 containing atmosphere but exhibit more than one order of magnitude lower proton conductivity than BaCeO3 based perovskites compounds [153]. The maximum conductivity 7.5×10^{-4} S/cm was observed for Ca doped Gd_2O_3 (900°C).

Acceptor-doped rare earth phosphates, $LnPO_4$ ((Ln=La, Ce, Pr, Nd, Sm with the monoclinic monazite-type structure and Ln=Y with the tetragonal xenotime-type structure) form another class of CO_2 tolerant materials with appreciable proton

conductivity [74-78]. Sr doped LaP_3O_7 has been studied due to its relatively high conductivity and especially because the protonic conduction appeared to be dominating even under low $P(H_2O)$ conditions [154].

Acceptor-doped rare earth orthoniobates and orthotantalates, $LnNbO_4$ and $LnTaO_4$, have been recently investigated as more stable proton-conducting materials by Haugsrud and Norby [155.]. The proton conductivity is dominated in these materials in wet atmospheres and the highest conductivity was found for Ca-doped $LaNbO_4$ ~0.001 S/cm at 950 °C with $P(H_2O)$ = 0.025 Pa [153.]. Also La_3NbO_7 shows similar proton conduction [156]. These materials are proved to be stable in CO_2 containing atmosphere, thus they are interesting candidates to operate for example using reformed natural gas.

1.13.3 Proton-conducting oxides: application in fuel cells

The development of proton conducting oxides for the fuel cell have stranded by the conflict between high proton conductivity and chemical and electrochemical stability under fuel cell operating conditions i.e. acceptor-doped $BaCeO_3$ shows the highest proton conductivity but the long stability in water and CO_2 containing atmosphere becomes a problem [124, 126.]. The electrolytes based on $BaZrO_3$ exhibit good stability but the conductivity is not high. Additional problems are related to the insufficient knowledge and research on electrodes for these new fuel cells [17]. However, due to the advantages of proton-conducting oxides fuel cells at intermediate temperature, more and more research institutions and companies have devoted to research and development on the proton conducting oxide fuel cells.

Ito et al. [157] made a laboratory fuel cell with a 0.7 μm-thick, Y-doped $BaCeO_3$ electrolyte deposited on a Pd anode substrate (40 μm) and with a perovskite cathode. The cell exhibited high power densities 1.4 W/cm^2 at 600 °C and 0.9 W/cm^2 at as low as 400 °C. This performance is higher than typical polymer exchange fuel cells and as high as that of

high temperature SOFCs even though it is operated at intermediate temperatures but substantial lifetimes were not reported.

Meng et al. [158] reported the power density of the cell using 50 μm films of Gd doped BaCeO3 (BGCO) as electrolyte $La_{0.5}Sr_{0.5}CoO_3$-BGCO as cathode, Ni-BGCO ermets as anode is around 300 mW/cm^2 at about 700°C for industrial ammonia or H_2 as fuel. This work exhibits how the unstable $BaCeO_3$ may be used with a basic fuel such as ammonia. It is very interesting and promising for application in fuel cells.

Acceptor-doped mixed barium zirconate cerates $Ba(Zr,Ce)O_3$ have been investigated for their better stability of the zirconate combined with the better conduction of cerate but fuel cell tests have not given convincing results [159, 160].

1.14 Objective of present investigation

The main objective of the present investigation is to develop cost effective novel electrolyte material as a proton conductor for SOFC with high ionic conductivity at intermediate temperature range. For this purpose Strontium Cerate based roton conductor as electrolyte material has been chosen. It has been also purposed to study the structural and electrical properties and tried to establish a correlation between them. In order to meet the above objectives it has been planned to:

- To synthesize host perovskite $SrCeO_3$ and a few series of Na^+, Gd^{3+} and La^{3+} doped perovskite $SrCeO_3$ electrolyte material as a proton conductor by solid state techniques.
- To study the thermal behaviour of the as prepared and sintered samples using differential scanning calorimetry (DSC) and thermogravimetry (TG) analysis.
- To study the phase formation and the crystal structure of the prepared electrolyte material using powder X-ray diffraction technique.

- To determine the density and porosity of sintered samples using Archimedes' principle
- To study the effect of doping on temperature dependence of conductivity behaviour of prepared samples using complex plane impedance spectroscopy.
- To study the microstructure employing scanning electron microscopy (SEM) and its correlation to the conduction mechanism.
- To study the oxidations state of the ions and oxygen vacancies by X-ray photoelectron spectroscopy (XPS) and its effect on the conduction mechanism.